Zeitschrift: IABSE publications = Mémoires AIPC = IVBH Abhandlungen
Band: 36 (1976)

Artikel: Strength of axially loaded stiffened panels
Autor: Horne, M.R. / Narayanan, R.
DOI: https://doi.org/10.5169/seals-915

Nutzungsbedingungen
Die ETH-Bibliothek ist die Anbieterin der digitalisierten Zeitschriften auf E-Periodica. Sie besitzt keine Urheberrechte an den Zeitschriften und ist nicht verantwortlich für deren Inhalte. Die Rechte liegen in der Regel bei den Herausgebern beziehungsweise den externen Rechteinhabern. Das Veröffentlichen von Bildern in Print- und Online-Publikationen sowie auf Social Media-Kanälen oder Webseiten ist nur mit vorheriger Genehmigung der Rechteinhaber erlaubt. Mehr erfahren

Conditions d'utilisation
L'ETH Library est le fournisseur des revues numérisées. Elle ne détient aucun droit d'auteur sur les revues et n'est pas responsable de leur contenu. En règle générale, les droits sont détenus par les éditeurs ou les détenteurs de droits externes. La reproduction d'images dans des publications imprimées ou en ligne ainsi que sur des canaux de médias sociaux ou des sites web n'est autorisée qu'avec l'accord préalable des détenteurs des droits. En savoir plus

Terms of use
The ETH Library is the provider of the digitised journals. It does not own any copyrights to the journals and is not responsible for their content. The rights usually lie with the publishers or the external rights holders. Publishing images in print and online publications, as well as on social media channels or websites, is only permitted with the prior consent of the rights holders. Find out more

Download PDF: 23.10.2025

ETH-Bibliothek Zürich, E-Periodica, https://www.e-periodica.ch

Strength of Axially Loaded Stiffened Panels

Résistance de panneaux raidis comprimés

Traglast längsversteifter, zentrisch gedrückter Plattenfelder

M.R. HORNE
MA ScD CEng FICE FIStructE.

R. NARAYANAN
MSc DIC PhD CEng MICE MIStructE FIE.

University of Manchester

1. Strength of thin Plates in Compression

The theoretical elastic critical stress of an ideally flat rectangular plate, loaded uniformly in one direction is given by [1]:

$$\sigma_{cr} = \frac{k\,\pi^2\,E}{12(1-\nu^2)} \cdot \left(\frac{t}{b}\right)^2$$

where

E = modulus of elasticity.
ν = Poisson's ratio.
t = thickness of plate.
k = a constant depending on the support conditions and on the aspect ratio (a/b).
a = length of plate in the direction of applied stress.
b = width of plate.

Provided elastic behaviour persists, buckling at the critical load [2] is followed by a redistribution of in-plane (membrane) stresses, this having a stabilising effect [3]. As the lateral (buckling) deflections of the plate develop, the longitudinal stress ceases to be uniformly distributed and membrane stress components parallel to the dimension b also appear. The ultimate stress may, on account of the redistribution of membrane stresses, rise considerably above the elastic critical stress.

Theoretical solutions taking account of membrane stress redistributions and based on the large deflection theory for the post-buckling behaviour of plates have been developed but generally overestimate the strength [4]. A theoretical method of determining the "critical load" of a long orthotropic plate with longitudinal edges simply supported against out-of-plane displacements but free to move in the plane of the plate was put forward by Chapman and Falconer [5]. They obtained expressions for the elastic buckling and post-buckling characteristics of an initially deformed orthotropic plate (the initial deformations following the sine-wave form)

using an energy method [1]. RASLAN [6] has given an alternative treatment of the same problem. The treatment both of Chapman and Falconer and of Raslan are approximate. To the extent that they are both energy methods and are based on an assumed (sinusoidal) post-buckling mode they give upper bounds to the longitudinal stiffness of the plate. In Raslan's treatment, however, this is compensated for by the neglect of membrane shear stresses on planes parallel to the edges of the plate panel.

Both methods assume that the longitudinal edges can deflect in-plane. In plates stiffened at regular intervals by longitudinal stiffeners (Fig. 3), the individual plate panels buckle in a series of waves which have nodes at the lines of stiffeners. If the bending interaction between the plate panels and the stiffeners is ignored, the plate panels can then be regarded as simply supported against out-of-plane displacements along their longitudinal edges but due to symmetry, they will be restrained along these edges against in-plane displacement. This "restrained-in-plane" condition will cause the induction of normal stresses acting in the direction of the dimension b, and these stresses are found to increase the longitudinal stiffness of the plate panel in the post-buckling range.

The following is a treatment of the case for longitudinal edges of a plate restrained in-plane, following the same general approach as that of Raslan.

2. Assumptions

(i) The material of the plate is homogeneous, isotropic, elastic and perfectly plastic, the effect of strain-hardening being neglected.
(ii) All edges of the plate are held straight, both in-plane and out-of-plane, but are free from restraining or applied moments.
(iii) Membrane shear stresses on planes parallel to the edges of the plate panel are assumed to be zero. Hence, by equilibrium the longitudinal membrane stress is constant in the longitudinal direction, although it may vary in the transverse direction. Similarly, any transverse membrane stress will be constant in the transverse direction although it will vary in the longitudinal direction.
(iv) The number and length of half waves is the same in the post-buckling stage as at incipient buckling.
(v) The buckling shape in the post-buckled stage is sinusoidal, being therefore identical with the shape of the infinitely small buckles during incipient buckling.

3. Ideally flat Plate

The plate ABCD in Fig. 1 is initially flat, and the transverse edges AB and CD in the coordinate direction Y, kept straight in-plane, are induced by the applied load to approach by a uniform displacement e_x.

The longitudinal edges BC and DA are also kept straight but are unloaded. Before buckling takes place, the induced longitudinal stress σ_x will be uniform, of value $\frac{Ee_x}{a}$, while the transverse stress σ_y will be zero. When σ_x reaches the elastic

critical stress σ_{cr}, the plate buckles in a series of half-wavelengths s, the deflected form being given by

$$w = A \sin \frac{\pi x}{s} \sin \frac{\pi y}{b} \tag{1}$$

where

w = lateral deflection,

A = amplitude of buckling.

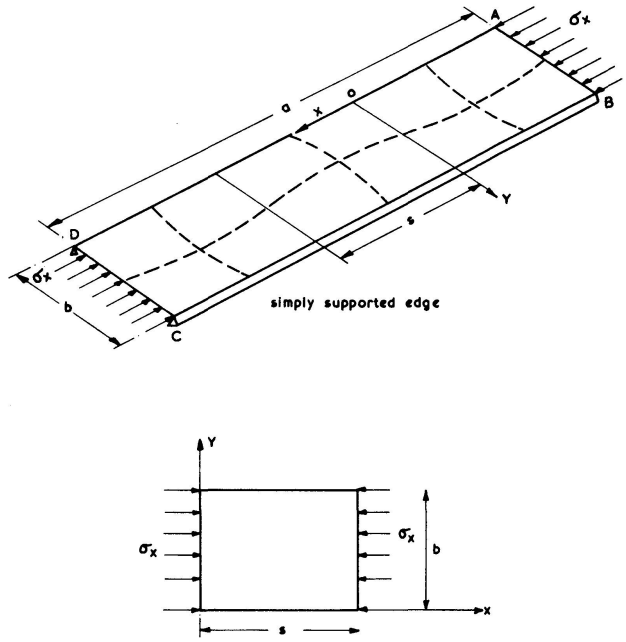

Fig. 1. Axial Loading on a simply supported Plate.

After buckling has occurred, the longitudinal stress σ_x will vary across the width of the plate, the Poisson expansion in direction OY being uniform along OX and of value $\frac{\nu}{E}\int_0^b \sigma_x dy$. In addition to this uniform expansion, there will be a uniform contraction e_y given by

$$e_y = \frac{\sigma_y b}{E} + \frac{A^2\pi^2}{4b} \sin^2 \frac{\pi x}{s} \tag{2}$$

where the second term on the r.h.s. is the flexural shortening due to the lateral deflection w given by (1).

Since the longitudinal edges are unloaded,

$$\int_0^s \sigma_y dx = 0 \tag{3}$$

Integrating equation (2) from 0 to s and using (3)

$$e_y = \frac{A^2\pi^2}{8b} \tag{4}$$

Hence, from (2),

$$\sigma_y = \frac{E}{b} \cdot \frac{A^2\pi^2}{8b} \cdot \cos\frac{2\pi x}{s} \tag{5}$$

Considering a half-wavelength of plate subjected in the post-buckling stage to stress σ_x, which varies across the width b, the internal strain energy U_{int} of the plate is obtained from the summation of energy due to bending U_b and the energy due to strain in the mid-plane of the plate U_s, i.e.

$$U_{\text{int}} = U_b + U_s$$

Due to symmetry in the assumed deflected form, the expression for bending energy for a half-wavelength reduces to

$$U_b = \frac{D}{2}\int_0^b\int_0^s \left(\frac{d^2w}{dx^2} + \frac{d^2w}{dy^2}\right)^2 dxdy$$

$$\text{where } D = Et^3/12(1-\nu^2)$$

Assuming that the deflected form remains the same as in the incipient buckling stage, the bending energy U_b may be derived by equating it to the external work done during elastic critical buckling, ignoring the effect of finite deformations. Hence

$$U_b = \frac{t}{2}\int_0^b\int_0^s \sigma_{cr}\left(\frac{dw}{dx}\right)^2 dxdy$$

Substituting for w from (1),

$$U_b = A^2K$$

where

$$K = \frac{\pi^2 t}{4s}\sigma_{cr}\int_0^b \sin^2\left(\frac{\pi y}{b}\right) dy \tag{6}$$

The energy U_s due to strain in the middle plane of the plate is given by

$$U_s = \frac{1}{2E}\int_0^b\int_0^s (\sigma_x{}^2 + \sigma_y{}^2 - 2\nu\sigma_x\sigma_y)\, t\, dxdy$$

$$= \frac{ts}{2E}\left(\int_0^b \sigma_x{}^2\, dy + \frac{\pi^4}{128}\cdot E^2 \cdot \frac{A^4}{b^3}\right)$$

Hence

$$U_{\text{int}} = A^2K + \frac{ts}{2E}\left(\int_0^b \sigma_x{}^2\, dy + \frac{\pi^4}{128}\cdot E^2\frac{A^4}{b^3}\right) \tag{7}$$

Any change in the amplitude from a finite value A to $(A + \delta A)$ caused by an applied additional mean longitudinal strain $d\varepsilon_x = \frac{de_x}{a}$ corresponds to a change in

the applied stress from σ_x to $(\sigma_x + d\sigma_x)$ and so, from (7) and substituting for K from (6), the change in the internal strain energy dU_{int} is obtained as

$$dU_{\text{int}} = \frac{AdA\pi^2 t}{2s}\sigma_{cr}\int_0^b \left(\sin^2\frac{\pi y}{b}\right)dy + \frac{ts}{E}\left(\int_0^b \sigma_x d\sigma_x dy + \frac{\pi^4 E^2}{64}\cdot\frac{A^3}{b^3}dA\right) \tag{8}$$

Let σ_{x1} be the applied stress beyond the critical stress σ_{cr} (i.e. $\sigma_{x1} = \sigma_x - \sigma_{cr}$). The shortening of the plate after reaching the critical stress σ_{cr} is the algebraic sum of the shortening caused by the stresses σ_{x1} and σ_y and also that caused by the flexural strain due to the lateral deflection, w.

The flexural shortening u can be calculated by substituting w from (1) in

$$u = \frac{1}{2}\int_0^s \left(\frac{dw}{dx}\right)^2 dx$$

Hence,

$$u = \frac{\pi^2 A^2}{4s}\cdot\sin^2\frac{\pi y}{b} \tag{9}$$

The longitudinal strain ε_{x1} beyond the strain at the critical stress σ_{cr} can be obtained by considering the axial shortening over the length s, i.e.

$$s\,\varepsilon_{x1} = s\cdot\frac{\sigma_{x1}}{E} - \int_0^s \nu\frac{\sigma_y}{E}\cdot dx + \frac{A^2\pi^2}{4s}\cdot\sin^2\frac{\pi y}{b}$$

But $\int_0^s \sigma_y dx = 0$, whence

$$\varepsilon_{x1} = \frac{\sigma_{x1}}{E} + \frac{A^2\pi^2}{4s^2}\cdot\sin^2\frac{\pi y}{b} \tag{10}$$

Due to a change in buckling amplitude dA and the accompanying changes $d\sigma_{x1}$ in the longitudinal stresses, (10) gives the value of the associated change in the longitudinal strain as

$$d\varepsilon_{x1} = \frac{d\sigma_{x1}}{E} + \frac{AdA}{2s^2}\pi^2\sin^2\frac{\pi y}{b} \tag{11}$$

Over the length s of the plate, the shortening is $sd\varepsilon_{x1}$. Hence the applied loads do work given by dT where,

$$dT = sd\varepsilon_{x1}\int_0^b \sigma_x\cdot t\cdot dy$$

Substituting for $d\varepsilon_{x1}$ from (11), we get

$$dT = \frac{st}{E}\int_0^b \sigma_x d\sigma_{x1}dy + \frac{AdA\pi^2 t}{2s}\int_0^b \sigma_x\cdot\sin^2\frac{\pi y}{b}dy \tag{12}$$

This increment of external work may be equated to the change of internal strain energy given by (8). After simplification and using

$$\sigma_{x1} = (\sigma_x - \sigma_{cr}), \text{ this leads to}$$

$$\int_0^b \sigma_{x1} \cdot \sin^2 \frac{\pi y}{b} \cdot dy = \frac{\pi^2}{32} E \left(\frac{sA}{b^2}\right)^2 b \tag{13}$$

Substituting for σ_{x1} from (10) and integrating the various terms, it is found that

$$\frac{\pi^2 A^2}{4s^2} = \frac{4\,\varepsilon_{x1}}{3 + \left(\frac{s}{b}\right)^4} \tag{14}$$

Substituting into (10),

$$\sigma_{x1} = (\sigma_x - \sigma_{cr}) = E\,\varepsilon_{x1} \left[1 - \left(\frac{4}{3 + \left(\frac{s}{b}\right)^4} \right) sin^2 \frac{\pi y}{b} \right] \tag{15}$$

For any longitudinal strain ε_{x1} beyond the strain at the critical stress, (14) gives the amplitude of the buckled form and (15) gives the distribution of the longitudinal stress σ_x. These equations define the behaviour of an ideally straight plate in the post-buckled elastic state. When the plate is subjected to increasing loads, the distribution of stresses remains uniform until it reaches the critical stress σ_{cr}; any additional increase of loads results in a non-uniform distribution of stresses given by (15). At the edges of the loaded sides, i.e. at $y = 0$ and $y = b$, the longitudinal boundary stress σ_e is obtained as

$$\sigma_e = \sigma_{cr} + E\,\varepsilon_{x1}$$

The increase of stress above the critical value is a minimum down the central axis, i.e. along $y = \frac{b}{2}$. The distribution of longitudinal stress is shown in Fig. 2.

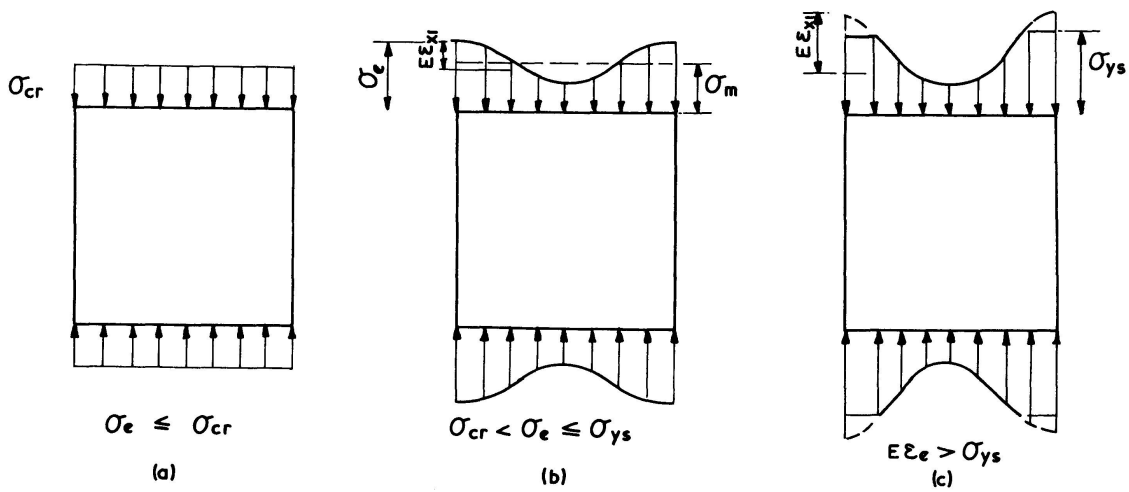

Fig. 2. Stress Distribution on a straight compressed Plate.

An infinitely long plate, or a plate of length nb (where n is an integer) will have the least value of initial buckling stress and will have a buckling half-wave-length of $s = b$. For such a plate,

$$\sigma_{cr} = \frac{\pi^2 E}{3(1-\nu^2)}\left(\frac{t}{b}\right)^2 \tag{16}$$

and the post-buckling distribution of longitudinal stress becomes

$$\sigma_x = \sigma_{cr} + E\,\varepsilon_{x1}\left(1 - \sin^2\frac{\pi y}{b}\right) \tag{17}$$

The mean longitudinal stress σ_m on such a plate is given by

$$\sigma_m = \sigma_{cr} + \frac{1}{b}\int_0^b \sigma_{x1}\,dy$$

i.e.

$$\sigma_m = \sigma_{cr} + 0.5\,E\,\varepsilon_{x1} \tag{18}$$

The transverse stress σ_y may be evaluated from (5) giving

$$\sigma_y = \frac{E}{b}\cdot\frac{A^2\pi^2}{8b}\cdot\cos\frac{2\pi x}{s}$$

Substituting for $\dfrac{A^2\pi^2}{4b^2}$ from (14), we obtain

$$\sigma_y = \frac{E}{2}\cdot\varepsilon_{x1}\cos\frac{2\pi x}{s} \tag{19}$$

4.1 *Simply supported Plates with initial Imperfections*

A theoretical analysis based on an ideally perfect plate is valuable only for determining the upper bound solutions. All plates, in fact, have some irregularity in their surfaces. While these irregularities follow no general pattern, it is usual to assume for the sake of simplicity that the initial imperfection of a plate is similar in form to the buckled shape of the plate. Thus the initial surface of the plate before any loads are applied can be expressed by an expression similar to (1), i.e.

$$w_0 = A_0 \sin\frac{\pi x}{s}\sin\frac{\pi y}{b} \tag{20}$$

where

w_0 = initial deflection function,
A_0 = amplitude of the initial wave,
s = half-wavelength of buckle.
The final buckled shape will be given by (1).

The lateral contraction e_y corresponding to a lateral compressive stress σ_y is given by

$$e_y = \frac{\sigma_y b}{E} + \frac{A^2 - A_0^2}{4b} \cdot \pi^2 \cdot \sin^2 \frac{\pi x}{s} \tag{21}$$

Since there is no restraint at the edges,

$$\int_0^s \sigma_y dx = 0$$

$$\text{Hence } e_y = \left(\frac{A^2 - A_0^2}{8b}\right) \pi^2 \tag{22}$$

By substitution in (21), we obtain

$$\sigma_y = \frac{E}{b}\left(\frac{A^2 - A_0^2}{8b}\right) \pi^2 \cos \frac{2\pi x}{s} \tag{23}$$

The energy stored in a half-wavelength is

$$U_b = (A - A_0)^2 K \tag{24}$$

where K is given by (6). The energy U_s due to strain in the mid-plane of the plate is obtained as for the initially flat plate, σ_y from (23) replacing the expression from (5), i.e. A^2 is replaced by $(A^2 - A_0^2)$.
Hence,

$$U_s = \frac{ts}{2E}\left[\int_0^b \sigma_x^2 \, dy + \frac{\pi^4}{128} \cdot E^2 \cdot \frac{(A^2 - A_0^2)^2}{b^3}\right] \tag{25}$$

The change in the total strain energy $U_{\text{int}} = (U_b + U_s)$ due to a small increment in the amplitude from A to $(A + dA)$ is obtained as

$$dU_{\text{int}} = 2(A - A_0)\, dA \cdot K + \frac{ts}{E}\int_0^b \sigma_x d\sigma_x dy + \frac{\pi^4}{64}\frac{tsE}{b^3} A(A^2 - A_0^2)\, dA \tag{26}$$

The longitudinal shortening due to an applied stress σ_x is obtained from

$$s\varepsilon_x = s \cdot \frac{\sigma_x}{E} - \frac{\nu}{E}\int_0^s \sigma_y dx + \frac{A^2 - A_0^2}{4s} \cdot \pi^2 \sin^2 \frac{\pi y}{b}$$

Since $\int_0^s \sigma_y dx = 0$,

$$\varepsilon_x = \frac{\sigma_x}{E} + \frac{A^2 - A_0^2}{4s^2} \cdot \pi^2 \sin^2 \frac{\pi y}{b} \tag{27}$$

whence,

$$d\varepsilon_x = \frac{d\sigma_x}{E} + \frac{A dA}{2s^2} \cdot \pi^2 \sin^2 \frac{\pi y}{b} \tag{28}$$

Over the length s of the plate, the shortening is $s \cdot d\varepsilon_x$ and the work done by the applied loads is

$$dT = \frac{st}{E}\int_0^b \sigma_x d\sigma_x \cdot dy + \frac{AdA\pi^2 t}{2s}\int_0^b \sigma_x \sin^2 \frac{\pi y}{b}\, dy \tag{29}$$

Using $dU_{\text{int}} = dT$, (26) and (29) give, after simplification,

$$\int_0^b [A(\sigma_x - \sigma_{cr}) + A_0\sigma_{cr}] \sin^2 \frac{\pi y}{b}\, dy = \frac{\pi^2 E s^2}{32b^3}(A^3 - AA_0{}^2)$$

Putting $m = \dfrac{A}{A_0}$, and rearranging the terms,

$$\frac{1}{Eb}\int_0^b [m(\sigma_x - \sigma_{cr}) + \sigma_{cr}] \sin^2 \frac{\pi y}{b}\, dy = \frac{\pi^2}{32}\cdot\frac{A_0{}^2 s^2}{b^4}(m^3 - m) \tag{30}$$

Considering the effect of an increment in amplitude represented by $dm = \dfrac{dA}{A_0}$,

$$\frac{1}{Eb}\int_0^b m d\sigma_x \sin^2 \frac{\pi y}{b}\, dy = \frac{\pi^2}{32}\cdot\frac{A_0{}^2 s^2}{b^4}(3m^2 - 1)\, dm - \frac{dm}{Eb}\int_0^b (\sigma_x - \sigma_{cr}) \sin^2 \frac{\pi y}{b}\, dy \tag{31}$$

Using $d\sigma_x$ derived from (28), equation (31) becomes

$$m\frac{d\varepsilon_x}{b}\int_0^b \sin^2 \frac{\pi y}{b}\, dy - \frac{\pi^2 A_0{}^2}{2s^2 b} m^2 dm \int_0^b \sin^4 \frac{\pi y}{b}\, dy$$

$$= \frac{\pi^2}{32}\cdot\frac{A_0{}^2 s^2}{b^4}(m^2 - 1)\, dm - \frac{dm}{Eb}\int_0^b (\sigma_x - \sigma_{cr}) \sin^2 \frac{\pi y}{b}\, dy \tag{32}$$

The last integral can be eliminated between (30) and (32) and after performing the integrations,

$$d\varepsilon_x = dm\left[\left(\pi^2 \cdot \frac{3}{8} \cdot \frac{A_0^2}{s^2} + \pi^2 \cdot \frac{A_0{}^2 s^2}{8 \cdot b^4}\right) m + \frac{\sigma_{cr}}{E}\cdot\frac{1}{m^2}\right]$$

Hence

$$\varepsilon_x = \frac{\pi^2}{16}\frac{A_0{}^2}{s^2}\left(3 + \frac{s^4}{b^4}\right)(m^2 - 1) + \frac{m-1}{m}\cdot\frac{\sigma_{cr}}{E} + C_1 \tag{33}$$

where C_1 is a constant of integration.
Under zero load, $m = 1$ when $\varepsilon_x = 0$, whence C_1 can be evaluated and

$$\varepsilon_x = \frac{\pi^2}{16}\cdot\frac{A_0{}^2}{s^2}\left(3 + \frac{s^4}{b^4}\right)(m^2 - 1) + \frac{m-1}{m}\cdot\frac{\sigma_{cr}}{E}$$

Designating $\dfrac{\pi^2 A_0{}^2}{4s^2}$ by ε_0 and $\dfrac{\sigma_{cr}}{E}$ by ε_{cr},

$$\varepsilon_x = \frac{m-1}{m}\varepsilon_{cr} + \varepsilon_0\left(\frac{3+\frac{s^4}{b^4}}{4}\right)(m^2-1)$$

When $s = b$, the above equation becomes

$$\varepsilon_x = \frac{m-1}{m}\varepsilon_{cr} + \varepsilon_0(m^2-1) \tag{34}$$

The stress at any section corresponding to an applied strain can be found by integrating (28), whence

$$\varepsilon_x = \frac{\sigma_x}{E} + \frac{A^2\pi^2}{4s^2}\cdot\sin^2\frac{\pi y}{b} + C_2$$

Here C_2 is a constant of integration which can be evaluated by putting $\sigma_x = 0$ when $\varepsilon_x = 0$ and $A = A_0$.
Hence it is found that

$$\sigma_x = E\left[\varepsilon_x - (m^2-1)\,\varepsilon_0\cdot\sin^2\frac{\pi y}{b}\right] \tag{35}$$

The mean stress then becomes

$$\sigma_m = E\left[\varepsilon_x - \frac{m^2-1}{2}\varepsilon_0\right] \tag{36}$$

From (23), σ_y can be expressed in terms of m and ε_0 as

$$\sigma_y = \frac{E}{2}(m^2-1)\,\varepsilon_0\cos\frac{2\pi x}{s} \tag{37}$$

4.2 *The Effective width of Plate*

The boundary stress σ_e is calculated directly from the longitudinal strain ε_x from $\sigma_e = E\,\varepsilon_x$. If the plate were initially flat and no buckling occurred, the longitudinal force at strain ε_x would be $(E\,\varepsilon_x\cdot b\cdot t) = \sigma_e\cdot bt$, but in a buckled plate is given by $\sigma_m\cdot b\cdot t = \sigma_e(K_{bs}\cdot b)\cdot t$ where K_{bs} is the secant effective width factor.
Hence,

$$\sigma_m = K_{bs}\cdot\sigma_e = K_{bs}\cdot E\,\varepsilon_x \tag{a}$$

Considering a plate having a buckle length $s = b$, σ_{cr} is given by (16) and ε_0 is defined by

$$\varepsilon_0 = \frac{\pi^2}{4}\frac{A_0{}^2}{b^2}$$

Eliminating b,

$$E\,\varepsilon_0 = \frac{3}{4}(1-\nu^2)\left(\frac{A_0}{t}\right)^2\sigma_{cr}$$

Using $\sigma_{cr} = E\,\varepsilon_{cr}$,

$$\varepsilon_0 = 4C\,\varepsilon_{cr} \tag{b}$$

where

$$C = \frac{3(1-\nu^2)}{16}\left(\frac{A_0}{t}\right)^2$$

It is readily shown from (34), (36), (a) and (b) that

$$K_{bs}\frac{\varepsilon_x}{\varepsilon_{cr}} = \frac{\sigma_m}{\sigma_{cr}} = \frac{m-1}{m}(1 + 2mC\,(m+1))$$

and

$$K_{bs} = \frac{1 + 2mC\,(1+m)}{1 + 4mC(1+m)} \tag{39}$$

This equation enables the effective width of a plate with initial imperfection A_0 (defined by C) and final deflection A (defined by $A = mA_0$) to be obtained.

5. Strength of Stiffened Panels

The present work arises out of the Interim Design Rules [7] drafted by the Merrison Box Girder Committee. The method is based on the effective width concept; in drawing up these rules, account was taken of the results of theoretical and experimental studies carried out by MOXHAM [8, 9] in which it was shown that residual stresses caused by longitudinal edge welds in a plate panel reduced its strength. These studies also showed that initial imperfections (spherical and transverse cylindrical type), even if small, have a marked influence on the strength of plates. (It should be noted that Moxham's theoretical and experimental studies were, however, confined to plates with longitudinal edges free in plane).

The criterion for the strength of a stiffened panel used in the Merrison Rules is the attainment of a boundary stress in the plate panel at which yield will occur (due to the combined membrane stresses and plate bending) anywhere in plate panel.

A method of design, alternative to the Merrison procedure, has been proposed as a result of studies conducted at Cambridge by several investigators during the past few years [10, 11, 12]. The method consists of obtaining the basic plate strength using Moxham's method [8] and the basic outstand strength and then treating the stiffened panel as a "wide column". A Perry-Robertson type of formula has been recommended for computing the panel strength. Charts applicable to panels with three ranges of welding shrinkage forces have been proposed.

While both methods represent advances in the treatment of the subject, both are somewhat conservative as shown by the experiments conducted at Manchester [13]. The Merrison approach, although based on actual plate/stiffener bending theory and to this extent preferable to the recent Cambridge method, is conservative because initial yielding in the *extreme fibres* of the plate is too limited in its

effect on stiffeners to bring about collapse of the stiffened panel. An alternative criterion for the limiting plate panel conditions can be argued as follows.

Compressive buckling of a plate results in the shedding of the load from the centre of the plate towards the edges. With increasing plate deflections, the edges carry increasingly higher proportion of the applied compression. When the applied strain causes an edge stress (σ_e) equal to the yield point of the material (σ_{ys}), no more increase of stress is possible at the edges. The total compressive force at this stage (ignoring local "extreme fibre" yield in the plate) will be $\sigma_{ys} \cdot K_{bs} \cdot bt$. Any further increase of strain will cause a reduction in the effective width consequent on (1) the spread of plastic zones at the edges of the panel and (2) the increase in deflection at the centre of plate.

Although the mean stress on the most highly stressed plate panel of a stiffened panel may be capable of further increase beyond the compressive force $\sigma_{ys} \cdot K_{bs} \cdot bt$, it is arguable that the decreasing stiffness (effective width) of the plate panel which sets in at this stage will rapidly cause the failure of the entire stiffened panel. To allow approximately for this behaviour, it is therefore proposed to assume that, after yield on the boundary, the stiffness of a plate panel disappears entirely, the compressive force remaining constant at $\sigma_{ys} \cdot K_{bs} \cdot bt$. This causes progressive increases in the bending stresses in the stiffeners and a spread of plate panel failure along the column until a maximum load is reached and failure occurs.

The application of this criterion is explored in the following theory.

6. Initial Assumptions in Developing the Theory

The complete strength analysis even for the simplest case of a single simply supported plate taking full account of plasticity and large deflections (solved by MOXHAM [8]) involves enormous computational effort. For purposes of analysing the present problem, the following simplifiying assumptions are made so that the effect of varying some of the parameters can be evaluated without extravagant demands on computing facilities.

(i) All the earlier assumptions (used in analysing plates in compression) are also applicable in the following analysis.
(ii) The stiffened panel is assumed to be wide enough for it to be treated as a pin-ended column. The orthotropic plate action of the stiffened panel is not considered. The analysis is carried out on a single longitudinal stiffener and its associated width of plating.
(iii) The stiffener does not buckle locally. (This is not a reasonable assumption for panels failing by "stiffener failure".)
(iv) Plane sections of the stiffener remain plane and perpendicular to the neutral axis.
(v) Residual shrinkage force is concentrated on a small area at the junction of plate and stiffener.
(vi) The panel can be treated as an assembly of small elements and the moment and curvature are constant over the length of this element.
(vii) The slopes of the column everywhere are small.
(viii) Shear deformations are neglected.

(ix) Stress-strain curve for steel is of the ideal elasto-plastic form and is the same for both compression and tension. Strain hardening is neglected.
(x) No constraint has been given to the stiffened plate during welding, i.e. the effect of clamping, etc., during welding is negligible.

7. The Proposed Theory for Stiffened Panels

A stiffened panel sketched in Fig. 3 and loaded axially will now be considered. Referring to Fig. 4a, let δ_0 be the initial plate imperfection over a gauge length of b *before* welding. Due to the application of heat during welding let this imperfection increase to $\delta_r = m\delta_0$. When the plate bends, the stiffener rotates such that it continues to remain normal to the plate at the plate/stiffener junction.

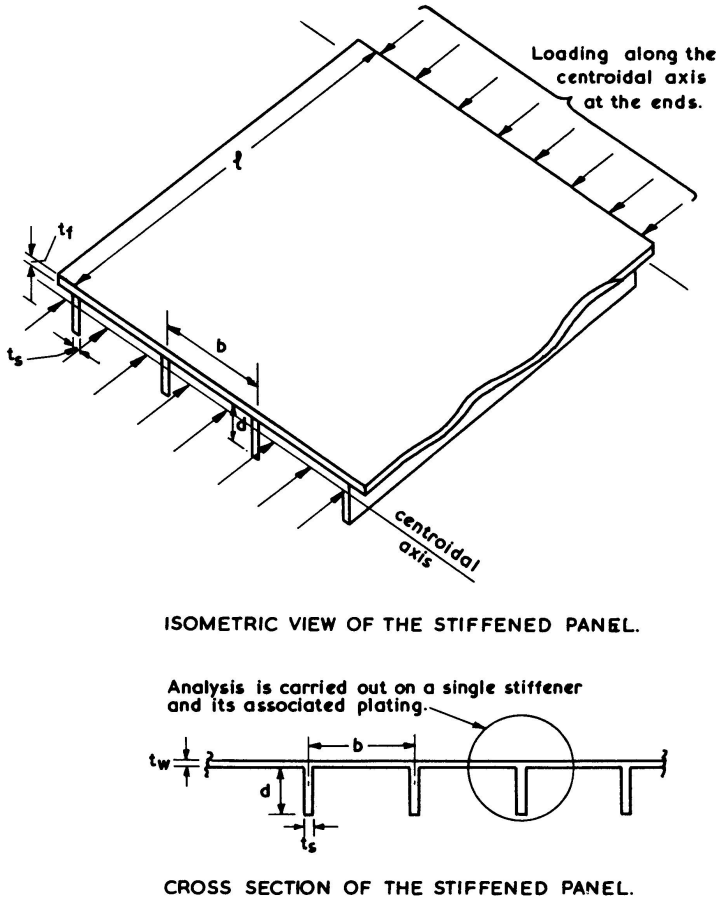

Fig. 3. Stiffened Panel.

As before, let the plate-deflection function be represented by

$$w = m\delta_0 \cdot \sin \frac{\pi y}{b} \sin \frac{\pi x}{s} \tag{40}$$

where

w = the vertical deflection of the plate at a distance y.
x is the longitudinal coordinate.
s is the half-wavelength of buckle.

At $y = 0$,

$$\frac{dw}{dy} = m\delta_0 \cdot \frac{\pi}{b} \cdot \sin \frac{\pi x}{s}$$

Assuming that the stiffener does not bend,

$$v = z \cdot \frac{m \cdot \delta_0 \pi}{b} \cdot \sin \frac{\pi x}{s}$$

where v is the lateral displacement of the stiffener at a depth z.
The flexural shortening in the stiffener

$$= \frac{1}{2} \int_0^s \left(\frac{dv}{dx}\right)^2 dx = \frac{\pi^4}{4} \cdot \left[\frac{m^2 \delta_0^{\,2}}{b^2 s^2} \cdot z^2\right] s$$

The unit flexural strain in the stiffener

$$= \frac{\pi^4}{4} \frac{m^2 \delta_0^{\,2}}{b^2 s^2} z^2 \tag{41}$$

Residual stress due to welding: Before welding, let the panel have an overall imperfection Δ_0 in the form of a circular arc. As a result of welding, let the overall imperfection increase to Δ_r over a gauge length (Fig. 4b).

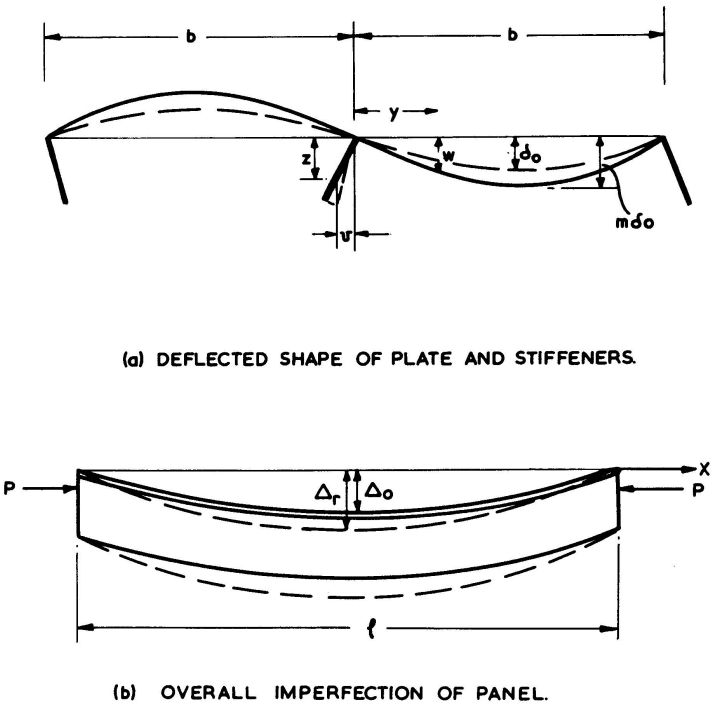

Fig. 4.

A stiffened panel, when welded together is subject to a residual shrinkage force caused by an area A_r under the tensile stress of σ_{ys} as sketched in Fig. 5a. To simplify the analysis, this condition is studied by adopting an idealised model con-

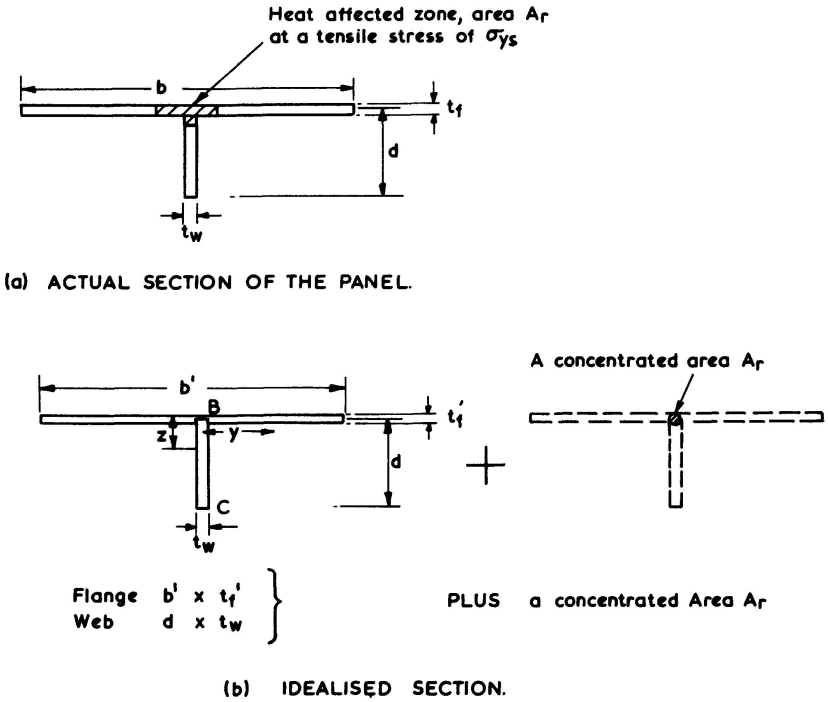

Fig. 5.

sisting of a concentrated area of A_r in tension plus a plate having a flange of $b' \times t'_f$ and a web of $d \times t_w$ (see Fig. 5b). The flange of the substitute panel is so chosen that

$$\frac{b}{t_f} = \frac{b'}{t'_f}$$

The total area of the actual panel and of the idealised model should be the same.

$$\text{i.e.} \left(d - \frac{t_f}{2}\right) t_w + bt_f = dt_w + b't'_f + A_r \tag{42}$$

$$\text{Let } \frac{b'}{b} = \frac{t'_f}{t_f} = \mu$$

$$\left(d - \frac{t_f}{2}\right) t_w + bt_f = dt_w + \mu^2 b \cdot t_f + A_r$$

Hence

$$\mu = \sqrt{1 - \frac{A_r + t_w \cdot \frac{t_f}{2}}{bt_f}} \tag{43}$$

Let the residual shrinkage force F_r change the initial plate imperfection from δ_0 to $m_r\delta_0$. Let the strain due to residual stress at the plate/stiffener junction (point B in Fig. 5b) be ε_r. The consequent mean stress in the flange $= K_r \cdot E\varepsilon_r$,

where K_r is the secant effective width factor when the "m" value for the plate is m_r. The values of m_r and ε_r may be related by putting $m = m_r$ and $\varepsilon_x = \varepsilon_r$ in (38).

Referring to Fig. 6b, the longitudinal strain at the tip of the stiffener (point C) $= \varepsilon_r - (\Delta_r - \Delta_0)\,\frac{8d}{l^2}$. At a distance z from the root of the stiffener,

$$\text{the longitudinal strain} = \varepsilon_r - (\Delta_r - \Delta_0)\,\frac{8z}{l^2} \tag{a}$$

This total longitudinal strain is composed of the flexural strain due to the warping of the stiffener parallel to the plate panel plus the strain due to the imposed residual stress.

The flexural strain in the stiffener is obtained from equation (41) where "m" changes from 1 to m_r

$$\text{i.e. Flexural strain} = \frac{\pi^4}{4}\,\frac{(m_r{}^2 - 1)}{b'^2 s^2}\cdot \delta_0{}^2 z^2 \tag{b}$$

Hence, the strain in the stiffener due to residual shrinkage is obtained by subtracting (b) from (a), i.e.

$$\varepsilon_{sr} = \varepsilon_r - (\Delta_r - \Delta_0)\,\frac{8z}{l^2} - \frac{\pi^4}{4}(m_r{}^2 - 1)\,\frac{\delta_0{}^2 z^2}{b'^2 s^2} \tag{44}$$

It has been assumed that there is no constraint given to the stiffened panel; hence the moment on the panel is zero.

$$\text{i.e.} \int_0^d z\cdot E\cdot \varepsilon_{sr}\cdot dz = 0$$

From equation (44),

$$\int_0^d \left[\varepsilon_r - (\Delta_r - \Delta_0)\,\frac{8z}{l^2} - \frac{\pi^4}{4}(m_r{}^2 - 1)\,\frac{\delta_0{}^2 z^2}{b'^2 s^2}\right] z\,dz = 0$$

whence

$$(\Delta_r - \Delta_0)\,\frac{8d^3}{3l^2} = \varepsilon_r\,\frac{d^2}{2} - \frac{\pi^4}{16}(m_r{}^2 - 1)\,\frac{\delta_0{}^2 d^4}{b'^2 s^2} \tag{45}$$

The longitudinal force in the stiffener is

$$S = E\cdot t_w \int_0^d \varepsilon_{sr}\,dz \tag{c}$$

The longitudinal force in the flange is

$$F = b' t'_f\, K_r\cdot E\cdot \varepsilon_r \tag{d}$$

The longitudinal force in the weld affected zone is

$$R = -\,A_r \sigma_{ys} \tag{e}$$

Since the net force on the section is zero, we may write

$$S + F + R = 0$$

Substituting $b' = \mu b$ and $t'_f = \mu t_f$,

$$Et_w \int_0^d \varepsilon_{sr} dz + \mu^2 K_r \cdot bt_f \cdot E\varepsilon_r - A_r \sigma_{ys} = 0$$

from which, using (44) and (45),

$$\left[\mu^2 \cdot \frac{bt_f}{dt_w} K_r + \frac{1}{4}\right] \varepsilon_r + \frac{\pi^4}{96}(m_r^2 - 1) \frac{\delta_0^2 d^2}{b'^2 s^2} - \frac{A_r}{t_w d} \cdot \frac{\sigma_{ys}}{E} = 0 \tag{46}$$

This equation together with (38) and (45) enables m_r, ε_r and Δ_r to be derived. Hence the residual stress distribution in the panel after welding can be derived.

7.1 *Load-deflection Relationship for the Panel*

The panel subjected to an axial load will now be considered (see Fig. 4a). At any stage in the loading cycle let the plate panel deflection be $m\delta_0$ and the corresponding strain at plate/stiffener junction be ε. Let an increase of strain at this position $= \delta\varepsilon$ correspond to an increase in plate deflection to $(m + \delta m)\delta_0$. Let the corresponding longitudinal plate stress at y (Fig. 6a) change from σ_x to $(\sigma_x + d\sigma_x)$. The change in the longitudinal force in the flange will then be

$$\delta F = t'_f \int_0^{b'} d\sigma_x dy \tag{47}$$

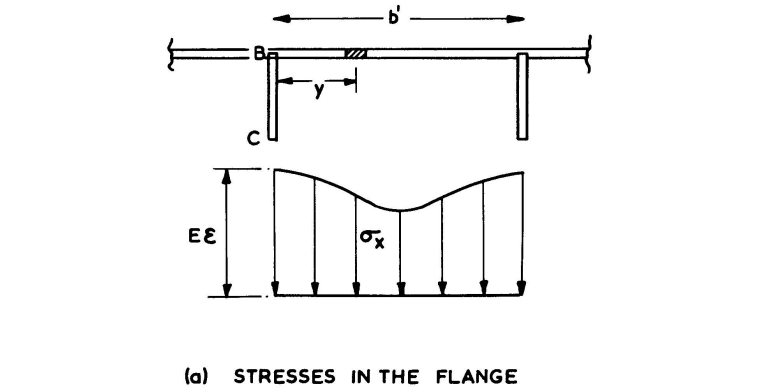

(a) STRESSES IN THE FLANGE

Fig. 6.

(b) STRESSES IN THE WEB.

Considering the stiffener (Fig. 6b), the total longitudinal strain at z is $\varepsilon - \left(\rho - \frac{8\Delta_0}{l^2}\right)z$ where ρ denotes the total curvature of the stiffened panel in a longitudinal plane.

Flexural strain at z is $\frac{\pi^4}{4}(m^2 - 1)\frac{\delta_0{}^2 z^2}{b'^2 s^2}$.

The longitudinal stress in the stiffener is elastic; the stress in the stiffener is therefore

$$\sigma_{xs} = E\,\varepsilon_s = E\left[\varepsilon - \left(\rho - \frac{8\Delta_0}{l^2}\right)z - \frac{\pi^4}{4}(m^2 - 1)\frac{\delta_0{}^2 z^2}{b'^2 s^2}\right] \tag{48}$$

whence

$$d\sigma_{xs} = E\left[\left(\frac{d\varepsilon}{dm} - \left\{\frac{\pi^4}{2}\right\} m\,\frac{\delta_0{}^2 z^2}{b'^2 s^2}\right) dm - z d\rho\right] \tag{49}$$

The change in longitudinal force in the stiffener is

$$\delta S = t_w \int d\sigma_{xs} dz \tag{50}$$

The change of moment about 00 (Fig. 6b) is

$$\delta M = t_w\,[\int z d\sigma_{xs} dz] \tag{51}$$

$$\text{Let } \delta S = \frac{dS_1}{dm}\cdot \delta m + \frac{dS_2}{d\rho}\cdot \delta\rho \tag{52}$$

$$\delta m = \frac{dM_1}{dm}\cdot \delta m + \frac{dM_2}{d\rho}\,\delta\rho \tag{53}$$

where

$$\frac{dS_1}{dm} = E t_w \int \left(\frac{d\varepsilon}{dm} - \frac{\pi^4}{2} m\cdot \frac{\delta_0{}^2 z^2}{b'^2 s^2}\right) dz \tag{54}$$

$$\frac{dS_2}{d\rho} = -\,E t_w \int z dz \tag{55}$$

$$\frac{dM_1}{dm} = E t_w \int \left(\frac{d\varepsilon}{dm} - \frac{\pi^4}{2} m\cdot \frac{\delta_0{}^2 z^2}{b'^2 s^2}\right) z dz \tag{56}$$

$$\frac{dM_2}{d\rho} = -\,E t_w \int z^2 dz \tag{57}$$

Also, from equation (47), we have, for the flange,

$$\frac{dF}{dm} = t'_f \int_0^{b'} \frac{d\sigma_x}{dm} dy \tag{58}$$

The change in the longitudinal force in the weld-affected zone is

$$\left(A_r \cdot E\,\frac{d\varepsilon}{dm}\right) dm \tag{59}$$

Let us consider the condition of the panel at some intermediate stage in the loading sequence. Let the axial force change from P to $(P + \delta P)$. Let the beam column be divided into j elements and let us consider the *nth* element (Fig. 7). Let the strain at the stiffener flange intersection change from ε_n to $(\varepsilon_n + \delta\varepsilon_n)$ and the curvature of the element from ρ_n to $(\rho_n + \delta\rho_n)$. At the commencement of loading, all elements have the same curvature given by

$$\rho = \frac{8}{l^2} \cdot \Delta_r \tag{60}$$

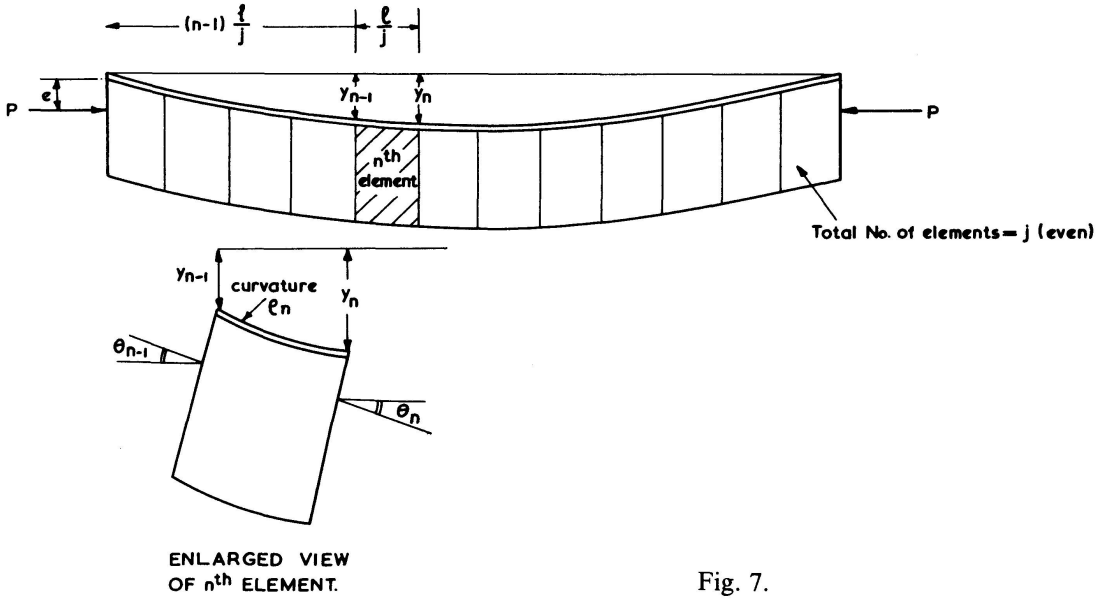

Fig. 7.

When there is an increment of load (from P to $P + \delta P$) we may write using (54), (55), (58) and (59)

$$\delta P = \left(\frac{dF}{dm_n} + \frac{dS_1}{dm_n} + A_r E \frac{d\varepsilon_n}{dm_n} \right) \delta m_n + \frac{dS_2}{d\rho_n} \delta\rho_n \tag{61}$$

where the subscript n refers to the quantities pertaining to the *nth* element.

The moment about the plate/stiffener intersection at the centre of the element is given by

$$(P + \delta P)\left(e - y_{n-1} - \frac{l}{2j} \cdot \theta_{n-1} + \frac{\rho_n}{8}\left(\frac{l}{j}\right)^2 \right) = M_n + \frac{dM_n}{dm_n} \cdot \delta m_n + \frac{dM_n}{d\rho_n} \delta\rho_n \tag{62}$$

There are thus two equations connecting δm_n and $\delta\rho_n$ to other known quantities in respect of each element, i.e. there are $2j$ equations for $2j$ unknowns. These can be solved to evaluate δm and $\delta\rho$ in respect of each element. The slope of each element is calculated by assuming that the curvature over the element is uniform

$$\text{i.e. } \theta_n = \theta_{n-1} - \rho_n \left(\frac{l}{j}\right) \tag{63}$$

$$y_n = y_{n-1} + \left(\frac{l}{j}\right) \theta_{n-1} - \frac{\rho_n}{2}\left(\frac{l}{j}\right)^2 \tag{64}$$

The "crushing load" of the panel (i.e. the load corresponding to a very small slenderness ratio), can be found by considering a short length of panel and applying a uniform load at ends until failure. (This corresponds to a short specimen tested in the "fixed-ended" condition.) In this case $\delta\rho_n = 0$ always. To obtain the crushing load of the panel, only equation (61) is used with $\delta\rho = 0$. It is also unnecessary to split the specimen into a number of strips along its length (i.e. $j = 1$).

$$\delta P = \left(\frac{dF}{dm} + \frac{dS_1}{dm} + A_r \cdot E\,\frac{d\varepsilon}{dm}\right)\delta m \tag{65}$$

Care should be taken to see that while computing $\frac{dF}{dm}$, $\frac{dS_1}{dm}$, $\frac{d\varepsilon}{dm}$, etc.,

$$|\sigma_x| \not> K_{bs}\sigma_{ys} \text{ and } |\sigma_{xs}| \not> \sigma_{ys}.$$

The procedure for computation is given in the Appendix.

8. Comparison with Test Results

The values of global average stress at failure observed in the laboratory on the various test panels will now be compared with the corresponding values predicted by using the theoretical treatment described in the foregoing pages; the important dimensions and details of these panels have been set out in Table 1. The detailed description of these tests will be found in two separate research reports [13, 16]. Observed test results on eight fixed-ended tests on short panels, and of ten pin-ended tests on panels having $l/r \simeq 90$ with the corresponding predicted values using (i) the proposed effective width theory and (ii) the Merrison Rules, are given in Tables 2 and 3. In these Tables, Column 2 gives the load at failure expressed as a fraction of the squash load. Column 3 gives the corresponding theoretical values, taking the residual shrinkage force acting on the panel as that obtained from Merrison Interim Design Rules. These are compared with the values obtained by taking the residual shrinkage force to be zero in Column 4. It will be seen that in all the cases, the theory predicts the strength of the panel to a reasonable degree of accuracy. It will also be noticed that there is only a small difference between the strengths predicted by allowing for residual shrinkage forces and those obtained by assuming zero residual stresses. The experiments also show that the ultimate strengths of these panels were influenced only marginally by the type of welding (and therefore by the magnitude of shrinkage forces).

Columns 5 and 6 give the predicted values using Merrison Rules; the former is obtained by introducing the residual shrinkage force as an additional imperfection, while the latter is obtained by using the shrinkage force as an additional stress to be accounted for in the computation. Merrison Rules provide that the more favourable of the two may be adopted; the corresponding values are shown in italics.

Table 1: Details of Panels Tested

Specimen No.	Plate thickness mm	Stiffener spacing mm	Stiffener size mm	Welding type	Imperfections in plate δ_x mm	Imperfections overall Δ_r mm
Fixed-ended tests (all panels 915 mm long)						
6	9.5	457	152 × 16	Continuous	0.8	≃ 0
1	9.5	457	152 × 16	Continuous	4.38	0
4	9.5	457	152 × 16	Intermittent	1.3	0
2	9.5	457	152 × 16	Intermittent	5.5	0
B11	6.5	457	152 × 9.5	Intermittent	5.9	0
B12	6.5	457	152 × 9.5	Intermittent	1.4	0
B21	6.5	457	152 × 9.5	Continuous	5.9	0
B22	6.5	457	152 × 9.5	Continuous	1.0	0
Pin-ended tests (all panels 1830 mm long)						
D11	10	457	80 × 12	Intermittent	5.4	1.4
D12	10	457	80 × 12	Intermittent	3.1	2.2
D21	10	457	80 × 12	Continuous	5.7	1.4
D22	10	457	80 × 12	Continuous	1.2	1.6
D23	10	457	80 × 12	Continuous	1.4	1.4 (ecc. load $e = 8$ mm)
E11	6.5	457	76 × 12.5	Intermittent	6.3	1.6
E12	6.5	457	76 × 12.5	Intermittent	1.7	1.6
E21	6.5	457	76 × 12.5	Continuous	5.6	1.9
E22	6.5	457	76 × 12.5	Continuous	1.3	2.7 (ecc. load $e = 8$ mm)
E23	6.5	457	76 × 12.5	Continuous	2.5	1.05

Table 2: Comparison of test results with the theoretically predicted strengths
(Fixed-ended tests)

Panel No.	Observed ultimate load / squash load	Predicted values of stress at failure/yield strength using: Proposed effective width theory: Res. stress acc. to Merrison Rules	Proposed effective width theory: $\sigma_R = 0$	Merrison Rules: Using σ_R as an imperfection	Merrison Rules: σ_R introduced as an addl. stress
6	0.92	0.82	0.95	*0.58*	0.55
1	0.87	0.77	0.82	*0.61*	0.44
4	0.90	0.92	0.92	0.57	*0.60*
2	0.83	0.80	0.80	*0.60*	0.55
B11	0.63	0.65	0.68	*0.62*	0.58
B12	0.65	0.69	0.72	*0.60*	0.49
B21	0.67	0.62	0.67	*0.64*	0.50
B22	0.62	0.63	0.72	*0.61*	0.38

Specimens 6, 1, 4 and 2 were made of 9.5 mm plates stiffened by 152.5 × 16 mm stiffeners; the first two were continuously welded, and the others intermittently welded. All the specimens were 915 mm long. Specimens 1 and 2 were "dished" to impose additional plate imperfections equal to 2½ to 3 times the Merrison tolerances. Specimens 6 and 4 were tested nominally straight.

Specimens B11, B12, B21 and B22 were made of 6.5 mm plates stiffened by 152.5 × 9.5 mm stiffeners; the first two were intermittently welded and the others were continuously welded. Specimens B12 and B22 were tested in the nominally straight condition while specimens B11 and B21 were tested after imposing additional plate imperfections by dishing. All specimens were 915 mm long.

The first five tests (D series) in Table 3 were performed on nominal ⅜″ (10 mm) plate panels stiffened by 3″ × ½″ (80 mm × 12 mm) flat stiffeners. The panels were made of Structural Grade 43 Steel. Specimens D11 and D12 were fabricated by employing intermittent welding (100 mm weld and 300 mm miss) to connect the plate and the stiffeners. Specimens D21, D22 and D23 were continuously welded. Specimens D12 and D22 were tested in the nominally straight state, while specimens D11 and D21 were "dished" to induce imperfections in the plate of magnitude equal to three times the Merrison tolerance. Specimen D23 was similar to D22, but was tested with the load applied at an eccentricity of 8 mm from its centroidal axis towards the plate. All the specimens were 72″ (1830 mm) long and tested in the pin-ended condition. The l/r for the specimens was 92.

Table 3: Comparison of test results with theoretically predicted strengths
(Pin-ended tests)

Spec. No.	Observed ultimate load / squash load	Predicted values of global average stress at failure/yield strength using			
		Proposed effective width theory		Merrison Rules	
		σ_R acc. to Merrison Rules	$\sigma_R = 0$	σ_R introduced as imperfection	σ_R introduced as an addl. stress
D11	0.63	0.57	0.58	*0.53*	0.48
D12	0.65	0.65	0.69	0.54	*0.58*
D21	0.57	0.57	0.61	*0.54*	0.40
D22	0.60	0.64	0.78	*0.52*	0.47
D23	0.43	0.43	0.45	*0.42*	0.37
E11	0.47	0.39	0.41	*0.49*	0.46
E12	0.48	0.46	0.48	*0.48*	0.42
E21	0.44	0.37	0.41	*0.49*	0.41
E22	0.34	0.32	0.36	*0.39*	0.27
E23	0.45	0.46	0.47	*0.50*	0.37

Specimens of the E series were made using "Corten" plates and grade 50 steel flats for stiffeners. The panels were made of nominal ¼″ (6.5 mm) thick plates and four 3″ × ½″ (76 mm × 12 mm) flat stiffeners. All the specimens were 72″ (180 mm) long and tested in the pin-ended condition. The l/r for the specimens was 88.

Specimens E11 and E12 were intermittently welded as in the D series, and E21, E22 and E23 were continuously welded. Specimens E12 and E23 were tested in the nominally straight condition, while specimens E11 and E21 were tested after dishing the plates to give imperfections of three times the Merrison tolerance. Specimen E22 was also tested in the nominally straight state with the axial load acting at an eccentricity of 8 mm towards the plate.

It will be seen from Tables 2 and 3 that the proposed theory predicts the strength of the panels within a reasonable degree of accuracy, the only exception

being D22, where the prediction was somewhat higher than the experimentally-recorded value. This panel failed suddenly by overall buckling immediately after the recorded maximum load, when an increment of axial strain was being applied to the specimen. Thus there is uncertainty about the actual maximum load (which was higher than the recorded value) as it could not be ascertained due to the sudden failure of the panel.

In general, the values predicted by the above theory, ignoring residual shrinkage forces, are not materially different from the values obtained by including their influence (compare Columns 3 and 4). On the other hand, the Merrison Rules predictions are generally very conservative except in the case of high b/t and high l/r, where these predictions are slightly higher than the observed values.

9. Comparison with Tests conducted at Monash University

The new theory developed above has also been checked against the experimental results obtained by MURRAY [14] at Monash University. Only tests on panels having $l/r \simeq 60$ have been chosen for comparison, as shorter panels tend to fail by crushing; the Rigid Plastic Analysis developed by Murray is adequate for the short panels.

The results obtained by him experimentally have been compared with the ultimate strengths computed from the above theory in Table 4. In deriving the strengths, it has been assumed that (a) the bulb flat stiffeners used by him may be substituted by flat stiffeners having the same area and (b) the influence of residual stresses

Table 4: Monash University tests

	Plate failure tests		Stiffener failure tests	
	Panel H	Panel U	Panel J	Panel T
b/t	54	63	54	62
Stiffener spacing (mm)	533.4	609.6	533.4	609.6
Plate thickness (mm)	9.86	9.66	9.96	9.8
Stiffeners used	6″ × 7.42 lb	4″ × 4.51 lb	6″ × 7.42 lb	4″ × 4.51 lb
Equivalent stiffener thickness (mm)	9.6	8.8	9.6	8.8
Length of panel (mm)	3450	1700	3450	1700
Eccentricity of loading (if any), mm	—	—	2,54 mm towards the stiffener	—
l/r	75.3	66.6	75.3	66.9
Global average stress at failure N/mm²	264.9	173.3	234.1	169.4
Observed $\frac{\text{ultimate load}}{\text{squash load}}$	0.70	0.59	0.63	0.45
Theoretically computed value for $\frac{\text{ultimate load}}{\text{squash load}}$	0.62	0.64	0.59	0.42

Notes: 1. Panels H, U and J were nominally straight. Panel T had an induced overall imperfection of 3.56 mm favouring "stiffener failure".
2. Panel J was tested with load applied eccentrically with respect to centroidal axis (e = 2.54 mm). All other panels were axially loaded.

may be ignored. The values of plate imperfection and overall imperfection have not been reported by Murray and these have been taken from a range of values quoted by MACLEOD [15]. It appears from the later's thesis that the imperfections have not been systematically measured, presumably because their work was directed at the application of rigid plastic theory developed by Murray. In spite of this serious limitation, it appears that the predicted values are reasonably close to the observed values.

10. Theoretically Calculated Curves

Applying the above theory, the sensitivity of the global average stress at failure of a short specimen (i.e. very low l/r) to the initial plate imperfections in the panel has been studied for a b/t ratio of 48, using two panel sizes. It will be seen from Fig. 8 that with the imperfections limited to the Merrison tolerance value, the reduction in the strength of the panel is predicted to be 16%. This appears to be the most important influence on the strength of the panel.

The sensitivity of global average stress at failure to the residual stress in the panel was studied for $b/t=48$ (Fig. 9). This shows that for normal panels with a moderate amount of welding, the above theory predicts that the residual stresses have only a very small effect on the failure load. Even when a high degree of welding is employed, it is perhaps sufficient to apply a reduction factor of 5% to 8% on the calculated ultimate stress to allow for any adverse effect of welding.

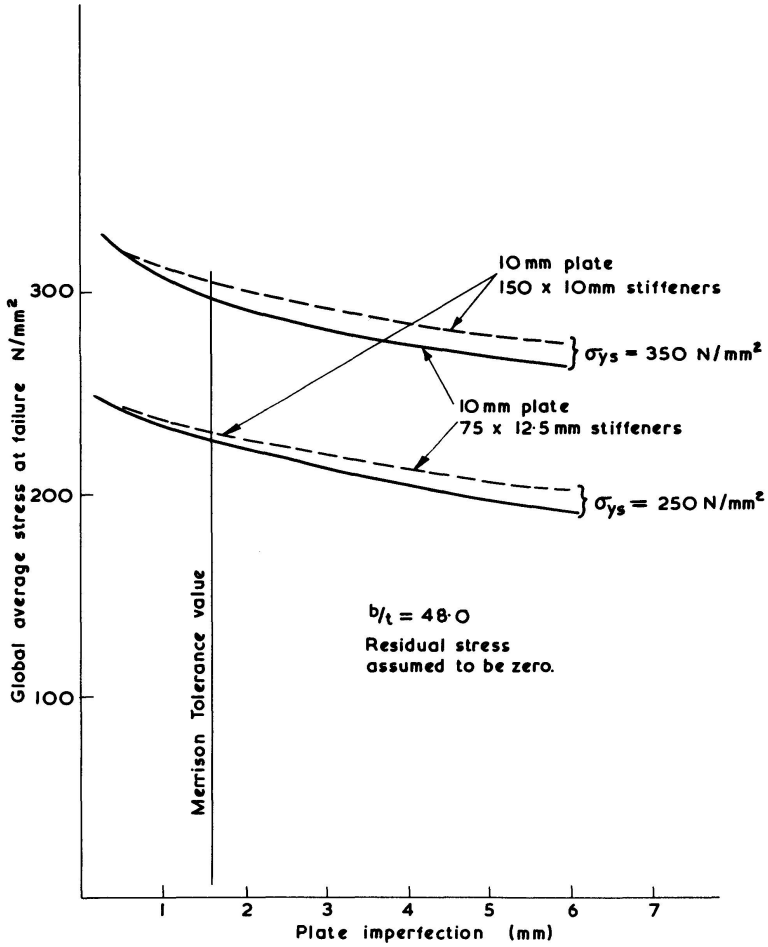

Fig. 8. Influence of Plate Imperfection on the Strength of Panel.

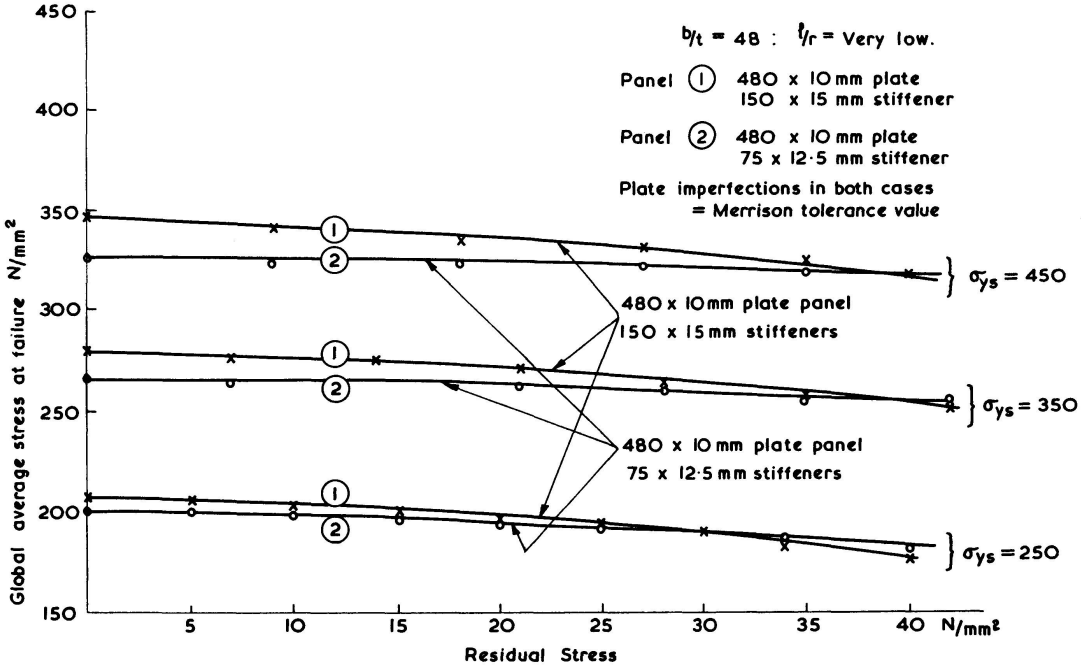

Fig. 9. The Influence of Residual Stress on the Ultimate Stress of Panel.

Fig. 10 is a study of b/t ratios on panel strengths which confirms what is already well-known viz that at values of b/t higher than about 40 the fall-off of strength is rapid.

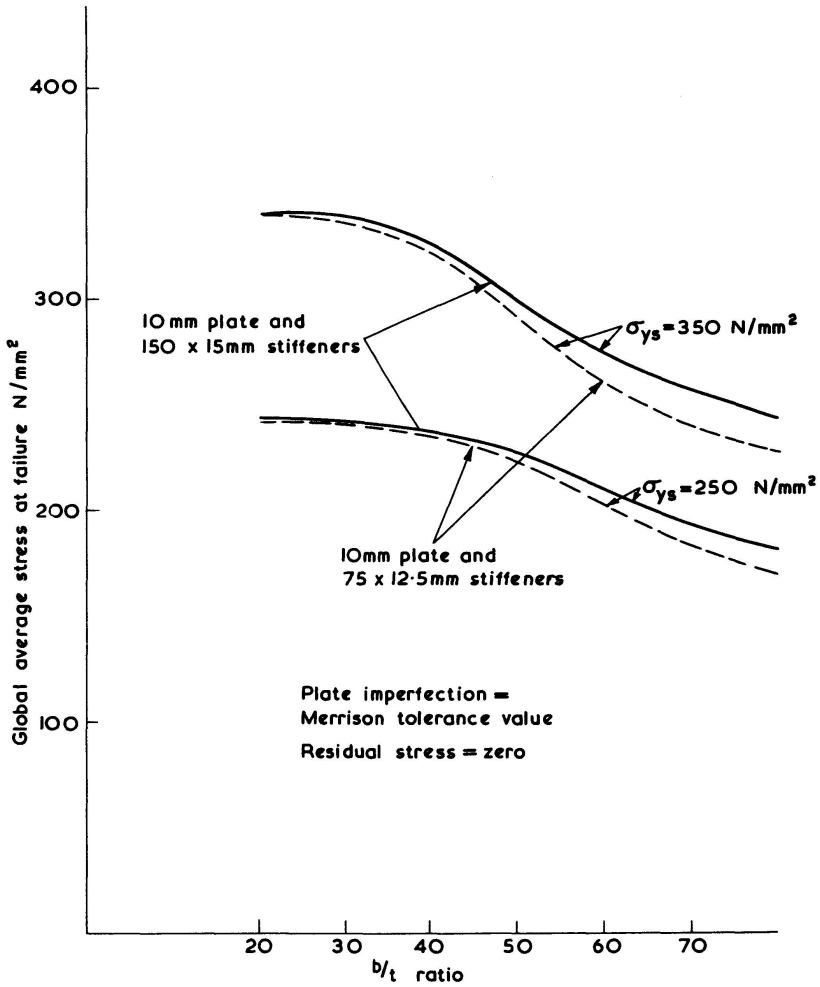

Fig. 10. Influence of b/t Ratio on the Strength of Panel.

11. Safety and Economy

The economic design of stiffened panels is affected not only by numerous design parameters (type of stiffener, section properties and spacing of stiffeners, thickness of flange plate) but also by the influence of fabrication procedures on residual stresses and imperfections, since these affect the strength and safety of the panel. These parameters have been tested experimentally at the Simon Engineering Laboratories of the University of Manchester, by carrying out load tests to collapse on a large number of stiffened panels, including variations in the welded connections between plate and stiffeners (thus affecting the residual stresses) and in initial imperfections of various types. Results from these tests have been used to check the validity of an analysis described in detail in the present paper.

Briefly stated, the analysis consists of determining at any mean longitudinal stress, the effective width of a plate for any given initial imperfection and obtaining the load-deflection path of a stiffened plate, using a step-by-step iteration process. Due allowance has been made for the initial imperfections of the plate, overall imperfections of the panel and residual shrinkage stresses due to welding.

The theory predicts and experiments confirm that

(i) the ultimate loads of these panels are affected only marginally by the type of welding (and therefore by the magnitude of the shrinkage forces).
(ii) Imperfections in plates have a high influence on the ultimate loads.
(iii) The Merrison Interim Design Rules for box girders are shown to be somewhat conservative for panels with low b/t and low l/r but may be unconservative for panels with high b/t and high l/r.
(iv) the method can be used to predict strengths of panels and so the optimum combination of plate thickness, stiffener size and spacing can be evaluated for an economic design.

12. Conclusions

An approximate solution for the problem of simply supported rectangular plates (restrained in-plane against in-plane displacement) under uniform compression in one direction has been obtained. This analysis avoids any tedious calculations which would become necessary when "large deflection theory" is used and can be easily applied even without the use of computers. The effective width of such a plate in compression has been derived.

Using the above concepts, a unified theory making allowance for initial imperfections and residual shrinkage force has been derived for stiffened panels under axial compression. Satisfactory predictions of ultimate strengths of stiffened panels have been obtained by using this theory (see Fig. 11).

The theory predicts and experiments confirm that residual shrinkage force due to welding has only a marginal influence on the strength of stiffened panels. On the other hand, an increase of plate imperfections results in a considerable reduction in the panel strength.

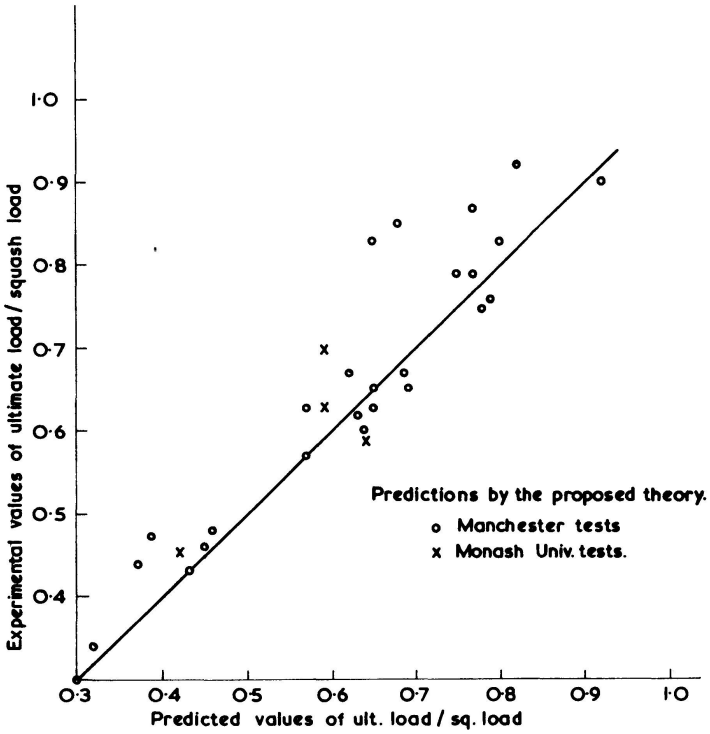

Fig. 11. Comparison of Experimental Results with the Theoretically Predicted Strengths.

13. Acknowledgements

The work has been supported by grants from the Science Research Council and the Construction Industry Research and Information Association.

The work has been carried out in the Simon Engineering Laboratories of the University of Manchester.

14. Appendix

Procedure for computation

A.1 *Steps in computation of residual stresses*

The residual shrinkage force at the plate/stiffener junction can be evaluated by any of the methods available; in these investigations, the formulae recommended by Merrison Interim Design Rules have been used. The point of application of this force is unknown, but it is reasonable to assume that this force is applied at B in Fig. 5b. The various steps involved in the computation are listed below:

(i) The residual shrinkage force (F_r) is computed using Merrison Rules.

(ii) μ, b', and t'_f corresponding to the idealised section are evaluated.

(iii) δ_0 is not yet known, but δ_x is obtained by direct measurement from the panel.

$$\delta_x = m_r \cdot \delta_0$$

To begin with, it is assumed that $m_r = 1$.

(iv) From the known values of m_r, δ_0, ε_0 and ε_r are computed:

$$\delta_0 = \delta_x / m_r$$

$$\varepsilon_0 = \frac{\pi^2 \delta_0^2}{4s^2}$$

$$\sigma_{cr} = \frac{\pi^2 E}{3(1-\nu^2)} \cdot \left(\frac{t'_f}{b'_f}\right)^2$$

$$\varepsilon_r = \left(\frac{m_r - 1}{m_r}\right) \cdot \left(\frac{\sigma_{cr}}{E}\right) + (m_r^2 - 1)\, \varepsilon_0$$

$$C = \frac{2.73}{16}\left(\frac{\delta_0}{t'_f}\right)^2 \quad (\text{taking } \nu = 0.3)$$

$$K_r = \frac{1 + 2m_r\, C\,(m_r + 1)}{1 + 4m_r\, C\,(m_r + 1)}$$

The above values are substituted in equation (46); the equation will be satisfied if our initial choice of m_r has been correct. (As it is, the initial guess for m_r would need improvement.) Let the error to be corrected (which is a function of m_r) be $f\,(m_r)$. This function should be made to converge to zero, by choosing a better value for m_r.

(v) As the next step, a small increment δm_r (say 0.00001) is given to m_r and the steps in (iv) are repeated with the new value for m_r. The difference between the two error functions is accounted for by the increase in m_r.
Let $\delta f = f(m_r + \delta m_r) - f(m_r)$
A better estimate for m_r can be obtained from choosing its new value as $m_r - \dfrac{f(m_r)}{(\delta f / \delta m_r)}$

(vi) $(\Delta_r - \Delta_0)$ and hence Δ_0 can now be computed from (45).

(vii) The stiffener is split into a large number of strips and ε_{sr} is computed from (44). The corresponding residual stresses σ_{sr} and the residual forces in all these strips are computed and added to obtain the residual force taken by the stiffener (F_s).

(viii) The plate is also split into a number of strips and the residual stresses in the plate corresponding to ε_r at B are then computed

$$\sigma_{pr} = E\left(\varepsilon_r - (m_r^2 - 1)\, \varepsilon_0 \cdot \sin^2 \frac{\pi y}{b'}\right)$$

The residual forces in all these strips are computed and summed up (F_p).

(ix) The total internal force is $(F_p + F_s)$ and would equal F_r, if the earlier choice of ε_r had been correct. If $F_0 = F_r - (F_p + F_s)$, then ε_r is the correct value when F_0 converges to zero.

(x) If $F_0 \neq 0$, than an increment $\delta\varepsilon_r$ is given to ε_r and steps (iv) to (ix) are repeated. Let the increase in F_0 be δF_0. The revised estimate for ε_r is

$$\varepsilon_r - \frac{F_0}{\dfrac{\delta F_0}{\delta\varepsilon_r}}.$$

The steps (iv) to (x) are now repeated to obtain the convergence of F_0 to zero.

(xi) The residual strains and stresses for this final value of ε_r are now stored in the computer memory.

A.2 *Computation of crushing load*

To begin with, ε_r is known at B from the previous computation. ε_{sr} is also known all along the stiffener. The residual strains and stresses in the elements of the plate and the stiffener have been stored in the computer memory. The value of m_r corresponding to ε_r is also known.

(i) A small longitudinal strain ε_B is uniformly applied across the whole section.

(ii) The total strain at B (Fig. 6a) $= \varepsilon_r + \varepsilon_B = \varepsilon$.

$$= \left(\frac{m-1}{m}\right) \cdot \left(\frac{\sigma_{cr}}{E}\right) + (m^2 - 1)\,\varepsilon_0$$

(This is a cubic equation and the solution is by trial and error.) The increment δm corresponding to the new value for ε is obtained.

(iii) A small increment Δm (say 0.000001) is applied to m and the corresponding $d\varepsilon$ and $\dfrac{d\varepsilon}{dm}$ is calculated.

(iv) The mean stress in the plate corresponding to the boundary strain ε is calculated from $K_{bs} \cdot E \cdot \varepsilon$. The maximum value of this stress is limited to $K_{bs} \cdot \sigma_{ys}$ (i.e. the stress at the edge of the plate is limited to σ_{ys}).

(v) Corresponding to $\delta\varepsilon$ from (iii), $\delta\sigma_x$ is calculated from (iv) and $\dfrac{d\sigma_x}{dm}$ is evaluated.

(vi) $\dfrac{d\sigma_x}{dm} \cdot t'_f \cdot b'$ is evaluated to give $\dfrac{dF}{dm}$.

(vii) The stresses in the stiffener are calculated from (48). The stress in the stiffener $\not> \sigma_{ys}$.

(viii) $E \cdot t_w \cdot \left(\dfrac{d\varepsilon}{dm} - \dfrac{\pi^4}{2} \cdot m \cdot \dfrac{\delta_0{}^2 \cdot z^2}{b^2 b'^2}\right) dz$ is evaluated for all the elements of the stiffener and added to give $\left(\dfrac{dS_1}{dm}\right)$.

(ix) $\left(A_r \cdot E \cdot \dfrac{d\varepsilon}{dm}\right)$ is computed with the condition that $E \cdot \varepsilon \cdot \not> 2\sigma_{ys}$ in order to avoid yield in compression in the heat-affected zone.

(x) The axial load (δP) corresponding to ε_B is

$$\delta P = \left(\frac{dF}{dm} + \frac{dS_1}{dm} + A_r \cdot E \cdot \frac{d\varepsilon}{dm} \right) \delta m$$

(xi) A further increment can now be given to ε_B and steps (ii) to (x) can be repeated.
The total axial load = load already applied + δP.
The computation is continued until all the elements have yielded.
The maximum load obtained is the crushing load.

A.3 *Computation procedure for pin-ended panels*

(i) The panel is divided into j elements along its length (Fig. 7). The values of deflections and mean curvature are computed for each element and stored in the computer.

(ii) The values of residual stresses across the section (previously computed) are applicable to each of the j elements.

(iii) $\frac{dF}{dm}, \frac{dS_1}{dm}, \frac{dS_2}{dm}, \frac{dS_2}{d\rho}, \frac{dM_1}{dm}, \frac{dM_2}{d\rho}$ and $\frac{d\varepsilon}{dm}$ are calculated for each of the elements; the restriction that the stress at any stiffener section should not exceed σ_{ys} and at any plate section, $K_{bs} \cdot \sigma_{ys}$ applies as before.

(iv) Equations (61) and (62) define δm_n and $\delta \varepsilon_n$ for each of the j elements corresponding to an applied load and the consequent deflection. (To begin with, the deflection at the centre is Δ_r and hence curvature of all the elements is $\frac{8\Delta_r}{l^2}$.)

(v) A small deflection $\delta\Delta$ is applied at the centre of the span and the corresponding load δP applied at the centroidal axis at the ends is guessed.

(vi) With this load δP, the moments in each of the j elements is evaluated from the left hand side of equation (62). At an intermediate stage in loading, the increase in moment δM_n due to an additional load δP is evaluated from

$$\delta M_n = (P + \delta P) \cdot \left[e - y'_{n-1} - \frac{l}{2j} \cdot \theta'_{n-1} + \frac{\rho'_n (l/j)^2}{8} \right]$$

$$- P \left[e - y_{n-1} - \frac{l}{2j} \theta_{n-1} + \frac{\rho_n (l/j)^2}{8} \right]$$

where

$y'_{n-1}, \theta'_{n-1}, \rho_n'$ refer to the values of deflection, slope and curvature after δP has been applied.

$y_{n-1}, \theta_{n-1}, \rho_n$ refer to the corresponding values when only the load P is acting along the centroidal axis at the ends.

(vii) The computations are started from the centre, where the slope is zero. From equations (61) and (62), δm_n and $\delta \rho_n$ are evaluated for each of the elements. The deflected shape of the panel can be traced using (63) and (64). If y_n at the right end is zero, then the guess value for δP (made in (v)) is correct.

(viii) If the guess value for δP is not correct, then steps (v) to (vii) are repeated (using Newton-Raphson Method) with improved values of δP, such that the y_n misclose at the right support is zero.

(ix) A further deflection can now be applied and steps (v) to (viii) are repeated.

Notation

a	length of the plate in the direction of applied stress.
A	amplitude of buckling wave.
A_0	initial imperfection in plate.
A_r	area of weld affected zone in tension.
b	width of plate.
b'	width of plate panel in the idealised model.
C	a constant $= \dfrac{3(1-\nu^2)}{16}\left(\dfrac{A_0}{t}\right)^2$.
d	depth of stiffener.
D	$Et^3/12(1-\nu^2)$.
e	eccentricity of applied load.
E	modulus of elasticity of the material of plate and stiffener.
e_x	uniform axial displacement in the x direction.
e_y	contraction in the y direction due to applied stress σ_x.
F	longitudinal force in the flange.
F_r	residual shrinkage force.
I	second moment of area of the idealised model.
j	number of elements along the length of the panel.
k	a constant (in the expression for critical load of plates).
K	a constant (U_b/A^2).
K_r	secant effective width due to residual shrinkage force.
K_{bs}	secant effective width of plate.
l	length of panel.
m	magnification ratio A/A_0.
m_r	the value of 'm' when plate deforms due to welding.
P	axial force in the panel.
r	radius of gyration of a stiffener and the associated width of plating about the centroidal axis.
R	longitudinal force in the weld affected zone.
s	half wavelength of buckling.
S	longitudinal force in the stiffener.
t_f	thickness of flange in the stiffened panel.
t_f'	thickness of flange in the idealised panel.
t_w	thickness of stiffener.
t	thickness of plate.
U_{int}	internal strain energy.
U_b	strain energy due to bending.
U_s	strain energy due to strain in mid-plane of plate.
u, v, w	displacements in x, y, z directions.

y_p	width of plastic zone in plate.
$\bar{y}$	distance of centroid of idealised model.
ν	Poisson's ratio.
ε_r	strain due to residual stress.
ε_B	strain at the junction of plate and stiffener.
ε_x	longitudinal strain due to applied stress σ_x.
ε_{x1}	longitudinal strain beyond the strain at critical stress σ_{cr}.
ε_{cr}	σ_{cr}/E.
ε_n	strain at the junction of plate and stiffener in the *nth* element.
δ_0	initial plate panel imperfection before welding.
Δ	increase of plate panel imperfection due to welding.
Δ_0	overall imperfection in the stiffened panel before welding.
Δ_r	overall imperfection in the stiffened panel after welding.
σ_{cr}	critical load of plate panel.
σ_e	longitudinal stress at the boundary of the plate.
σ_m	mean longitudinal stress in the plate.
σ_x	longitudinal stress applied to the plate in the x direction.
σ_{x1}	$(\sigma_x - \sigma_{cr})$.
σ_{xs}	stress in the stiffener.
σ_y	transverse stress.
σ_{ys}	yield point of steel.
μ	$\frac{b'}{b} = \frac{t_f'}{t_f}$.
ρ	initial curvature due to Δ_0.
ρ_n	curvature of element n.

16. References

1. TIMOSHENKO, S., and GERE, J.: Theory of Elastic Stability. 2nd Edition, McGraw Hill, 1961.
2. VON KARMAN, T., SECHLER, E.E., and DUNNEL, L.H.: Strength of thin Plates in Compression. Transactions of the American Society of Mechanical Engineers, J. of Appl. Mech., 54, p. 53, 1932.
3. BLEICH, F.: Buckling Strength of Metal Structures. McGraw Hill, 1952.
4. WINTER, G.: Strength of thin Steel Compression flanges. Transactions of the American Society of Civil Engineers, 2305, p. 527.
5. FALCONER, B.H., and CHAPMAN, J.C.: Compressive buckling of Stiffened Plates. The Engineer, June, 5 and 12, 1953, pp. 789-822.
6. RASLAN, R.A.S.: The Structural behaviour of Corrugated Plates. Ph. D. Thesis, University of Manchester, 1969.
7. Inquiry into the Basis of Design and Method of Erection of Steel Box Girder Bridges. Report of the Committee, Appendix I, Interim Design and Workmanship Rules, February 1973.
8. MOXHAM, K.E.: Theoretical Prediction of the Strength of welded Steel Plates in Compression. Cambridge University Engineering Department Report C-Struct/TR2, 1971.
9. MOXHAM, K.E.: Buckling Tests on individual welded Steel Plates in Compression, Cambridge University Engineering Department Report C-Struct/TR3, 1971.
10. DWIGHT, J.B., LITTLE, G.H., and ROGERS, N.A.: An Approach to stiffened Steel Compression Panels. Cambridge University Engineering Department Report CUED/C-Struct/TR32, 1973.
11. ROGERS, N.A.: Outstand failure in Stiffened Steel Compression Panels. Cambridge University Engineering Department Report No. CUED/C-Struct/TR34, 1973.
12. LITTLE, G.H.: Plate failure in Stiffened Steel Compression Panels. Cambridge University Engineering Department Report No. CUED/C-Struct/TR33, 1973.

13. HORNE, M.R., and NARAYANAN, R.: Ultimate load Capacity of Stiffened Panels. Report of the Simon Engineering Laboratories, University of Manchester, January 1974.
14. MURRAY, N.W.: Buckling of Stiffened Panels loaded axially and in bending. Structural Engineer, Vol. 51, August 1973.
15. MACLEOD, K.C.: The Behaviour of longitudinally Stiffened Steel Plate Panels. M.Sc. Thesis, Monash University, February 1973.
16. HORNE, M.R., and NARAYANAN, R.: Further Tests on Ultimate Capacity of Stiffened Panels. Report of the Simon Engineering Laboratories, University of Manchester, July 1974.

Summary

An approximate solution for the effective widths of simply supported rectangular plates under uniform axial compression in one direction has been presented. Using this concept, a unified theory making allowance for initial imperfections and residual shrinkage force has been derived for stiffened panels under axial compression. Test results of stiffened plates loaded axially show that the proposed theory accurately predicts the collapse loads.

Résumé

Les auteurs présentent une solution approximative pour déterminer la largeur effective des plaques rectangulaires simplement appuyées, soumises à une compression uniforme dans une direction. Partant de cette base, on établit une théorie générale, tenant compte des déflexions initiales et des contraintes résiduelles, pour l'étude des panneaux raidis comprimés. Les résultats d'essais entrepris sur des plaques de ce type montrent que la théorie proposée prédit exactement les charges de ruine.

Zusammenfassung

Die Autoren entwickeln eine Näherungslösung für die Bestimmung der mitwirkenden Breite rechteckiger längsgedrückter Platten mit gelenkig gelagerten Rändern. Diese Grundlage dient der Ableitung einer vereinheitlichten Theorie für die Untersuchung längsversteifter, zentrisch gedrückter Plattenfelder; dabei wird der Einfluss der anfänglichen Auslenkungen und der Schrumpfspannungen berücksichtigt. Versuche an solchen Plattenfeldern zeigen, dass sich mit der vorgeschlagenen Theorie die Traglast genau voraussagen lässt.

Leere Seite
Blank page
Page vide